

Binding between two-component bosons in one dimension

Emmerich Tempfli,¹ Sascha Zöllner,^{1,*} and Peter Schmelcher^{1,2,†}

¹Theoretische Chemie, Universität Heidelberg, Im Neuenheimer Feld 229, 69120 Heidelberg, Germany

²Physikalisches Institut, Universität Heidelberg, Philosophenweg 12, 69120 Heidelberg, Germany

(Dated: February 26, 2009)

We investigate the ground state of one-dimensional few-atom Bose-Bose mixtures under harmonic confinement throughout the crossover from weak to strong inter-species *attraction*. The calculations are based on the numerically exact multi-configurational time-dependent Hartree method. For repulsive components we detail the condition for the formation of a molecular Tonks-Girardeau gas in the regime of intermediate inter-species interactions, and the formation of a molecular condensate for stronger coupling. Beyond a critical inter-species attraction, the system collapses to an overall bound state. Different pathways emerge for different particle numbers and intra-species interactions. In particular, for mixtures with one attractive component, this species can be viewed as an effective potential dimple in the trap center for the other, repulsive component.

PACS numbers: 03.75.Mn, 67.60.Bc, 67.85.-d

I. INTRODUCTION

Cold atoms have become an important tool to create and study strongly correlated quantum systems [1, 2]. One main reason is that it is possible to experimentally tune the effective low-energy interaction strength between the atoms using Feshbach resonances [3]. This has been proven useful particularly for Fermi gases [4], whereas for bosons the creation of strong interactions is limited by three-body collisions. However, in lower (here: one) dimensions there are also other possibilities of achieving effectively strong correlations – e.g., by lowering the atom-number density [5] and via confinement-induced resonances, which exploit the parametric dependence on the transverse trapping potential [6]. This allows one to practically adjust the coupling strength all the way from infinitely attractive to hard-core repulsion.

For *single-component* bosons in one dimension (1D), the extreme case of infinitely repulsive interactions is known as the Tonks-Girardeau gas, which has been realized experimentally [7, 8]. Here the system maps to an ideal gas of fermions, in the sense that the exclusion principle emulates the effect of hard-core repulsion [9]. The microscopic mechanism of the crossover from the weakly interacting Bose gas to the above *fermionization* limit has been investigated in detail [10, 11, 12, 13, 14, 15]. By contrast, the ground state for strong *attraction* is an N -atom molecule [16]. However, exotic fermionized excitations exist for sufficiently attractive interactions [17, 18, 19].

In the case of *two* (or more) bosonic components, a plethora of configurations exists: On top of varying both intra- and inter-species interactions, also the trapping potentials may be made species dependent. Moreover, the experimental availability of different two-component mixtures (involving not only different hyperfine components [20, 21] or isotopes [22, 23], but altogether different atomic species like K-Rb [24]) adds another degree of flexibility. For two 1D Bose

gases with inter-species *repulsion*, a generalized, composite fermionization exists which may lead to demixing of the two components atom by atom [25, 26, 27, 28]. In a lattice potential, even more complex patterns have been found, cf. [29, 30, 31, 32] and Refs. therein.

In this work, we are interested in the *binding* between two bosonic species, i.e., the crossover from weak to strong inter-species *attraction*. Here little is known except for a general classification based on the harmonic-fluid approximation [33]. For *fermions*, pairing between the two components has been predicted, which then form a Tonks-Girardeau gas of molecules [34]. Similarly, pairing has been found to occur in attractive Bose-Fermi mixtures in various settings [35, 36, 37]. While, in principle, a 1D fermionic component maps to a strictly fermionized bosonic one, the physics of realistic Bose-Bose mixtures differs in two ways: For one thing, the finite intra-species repulsion must compete with strong inter-species attraction. More generally, in contrast to fermions all possible *intra-species* interactions are allowed and make for interesting phases. The key goal of this work is to demonstrate effects due to the interplay between intra-species and inter-species forces.

Our paper is organized as follows. Section I introduces the model and briefly reviews the computational method. The pairing between repulsive components is elucidated in Sec. II, first for the case of a mixture of balanced components (Sec. II A, II B), complemented by a discussion of atom-number imbalances and unequal intra-species interactions (Secs. II C). Section III deals with the question of how the presence of attractive components alters the picture. Model and computational method

Model The object of investigation is a two-component Bose gas (denoted $\alpha \in \{A, B\}$) subjected to a one-dimensional confinement, provided that the potentials acting on the different species are the same, i.e. $U_\alpha(x_A) = U(x_A)$ and $U_\alpha(x_B) = U(x_B)$. The two species can be considered as two internal states (pseudospin $|\uparrow\rangle$ and $|\downarrow\rangle$) of the same kind of Bose atoms with the mass $m = m_\alpha$. In the subsequent sections we denote the atom number of each species with N_α and the total number with $N = N_A + N_B$. This kinematically one-dimensional system of trapped bosons can be described in

*Electronic address: sascha.zoellner@pci.uni-heidelberg.de

†Electronic address: peter.schmelcher@pci.uni-heidelberg.de

the low-energy limit by the effective one-dimensional Hamiltonian with contact interactions. The second quantized Hamiltonian H then reads

$$H = \int dx \sum_{\alpha=A,B} \left\{ \hat{\Psi}_\alpha^\dagger(x) \left[-\frac{1}{2} \frac{\partial^2}{\partial x^2} + U(x) \right] \hat{\Psi}_\alpha(x) + \frac{g_\alpha}{2} \hat{\Psi}_\alpha^\dagger(x) \hat{\Psi}_\alpha^\dagger(x) \hat{\Psi}_\alpha(x) \hat{\Psi}_\alpha(x) \right\} + g_{AB} \int dx \hat{\Psi}_A^\dagger(x) \hat{\Psi}_B^\dagger(x) \hat{\Psi}_B(x) \hat{\Psi}_A(x), \quad (1)$$

where the field operator $\hat{\Psi}_\alpha(x)$ ($\hat{\Psi}_\alpha^\dagger(x)$), which annihilates (creates) a boson of the α -species at the position x . The effective intra- and inter-species couplings g_α and g_{AB} characterize the interaction between the atoms and can be controlled experimentally by the scattering lengths $a_0^{(\alpha)}$ and $a_0^{(AB)}$, respectively, in analogy to the single species case [6]. Furthermore, the standard rescaling procedure to harmonic oscillator units has been carried out (cf. [26] for details). For technical reasons we apply the Hamiltonian in the first quantized form. The eigenvalue problem reduces to solving the stationary Schrödinger equation $H\Psi = E\Psi$, with $H \equiv \sum_\alpha H_\alpha + H_{AB}$ composed of the single species Hamiltonian

$$H_\alpha = \sum_{i=1}^{N_\alpha} \left[\frac{1}{2} p_{\alpha i}^2 + U(x_{\alpha i}) \right] + \sum_{i < j} g_\alpha \delta_\sigma(x_{\alpha i} - x_{\alpha j})$$

and the inter-species coupling part

$$H_{AB} = \sum_{i=1}^{N_A} \sum_{j=1}^{N_B} g_{AB} \delta(x_{A_i} - x_{B_j}).$$

The effective two-particle interaction potentials in the low-energy region are $g_\alpha \delta_\sigma(x)$ and $g_{AB} \delta_\sigma(x)$ [6], which resemble a one-dimensional contact potential, but are mollified with a Gaussian $\delta_\sigma(x) \equiv e^{-x^2/2\sigma^2}/\sqrt{2\pi}\sigma$ (of width $\sigma = 0.05$) for numerical reasons (cf. [12] for details.) In the further examination we focus on the case of a harmonic confinement, $U(x) = \frac{1}{2}x^2$ and on attractive inter-species forces $g_{AB} \in (-\infty, 0]$. (The case of repulsive inter-species couplings has already been investigated in [26]. Note that, in the case of $U = 0$ and $g_\alpha = g_{AB}$ this system is integrable via Bethe's ansatz as in [5].)

Computational method Our approach relies on the numerically exact multi-configuration time-dependent Hartree method [38, 39, 40], a quantum-dynamics approach which has been applied successfully to systems of few identical bosons [12, 13, 19, 41, 42, 43] as well as to Bose-Bose mixtures [26]. Its principal idea is to solve the time-dependent Schrödinger equation $i\dot{\Psi}(t) = H\Psi(t)$ as an initial-value problem by expanding the solution in terms of direct (or Hartree) products $\Phi_J \equiv \varphi_{j_1}^{(1)} \otimes \dots \otimes \varphi_{j_N}^{(N)}$:

$$\Psi(t) = \sum_J A_J(t) \Phi_J(t). \quad (2)$$

The unknown single-particle functions $\varphi_j^{(\kappa)}$ ($j = 1, \dots, n_\kappa$) are in turn represented in a fixed basis of, in our case,

harmonic-oscillator orbitals. The specific feature of the system at hand is the indistinguishability within each species. Therefore the single-particle functions are identical within each subset $K_A = \{1, \dots, N_A\}$ and $K_B = \{N_A + 1, \dots, N\}$ (i.e. $\varphi_j^{(\kappa)} = \varphi_j^{(\alpha)}$, $\forall \kappa \in K_\alpha$). The permutation symmetry within each subset is ensured by the correct symmetrization of expansion coefficients A_J .

Note that, in the above expansion, not only the coefficients A_J but also the single-particle functions φ_j are time dependent. Using the Dirac-Frenkel variational principle, one can derive equations of motion for both A_J , φ_j [38]. Integrating this differential-equation system allows us to obtain the time evolution of the system via (2). This has the advantage that the basis set $\{\Phi_J(t)\}$ is variationally optimal at each time t ; thus it can be kept relatively small.

Although designed for time-dependent studies, it is also possible to apply this approach to stationary states. This is done via the so-called *relaxation* method. The key idea is to propagate some wave function $\Psi(0)$ by the non-unitary $e^{-H\tau}$ (propagation in imaginary time.) As $\tau \rightarrow \infty$, this exponentially damps out any contribution but that originating from the true ground state like $e^{-(E_m - E_0)\tau}$. In practice, one relies on a more sophisticated scheme termed *improved relaxation*, which is much more robust especially for excitations. Here $\langle \Psi | H | \Psi \rangle$ is minimized with respect to both the coefficients A_J and the orbitals φ_j . The effective eigenvalue problems thus obtained are then solved iteratively by first solving for A_J with *fixed* orbitals and then 'optimizing' φ_j by propagating them in imaginary time over a short period. That cycle will then be repeated.

II. MIXTURE OF TWO REPULSIVE COMPONENTS

In this section we investigate two repulsive components ($g_\alpha > 0$) with increasing inter-species attraction $g_{AB} \in (-\infty, 0]$. We start with components of equal intra-species settings, such as equal intra-species interaction strengths, $g_A = g_B$, and particle numbers $N_A = N_B$ and discuss subsequently the changes in the system's behavior when relaxing these conditions.

A. Mixture of two fermionized components

The starting point is the highly repulsive limit of the components, i.e. two quasi-fermionized states within the two species with the inter-species interactions $g_A = g_B = 25.0$. For small inter-species attraction $g_{AB} = -0.001$ the system is well described by the uncorrelated product of two Tonks-Girardeau (TG) states $\Psi = \Psi_A \otimes \Psi_B$, where $\Psi_A = \Psi_B \approx |\Psi_0^F|$. (This means, the state of each species α in the high-interaction limit ($g_\alpha \rightarrow +\infty$) can be mapped to a non-interacting state Ψ_0^F of identical fermions [9]. The limit case of infinite repulsion is commonly termed *fermionization* or *Tonks-Girardeau* state. By extension, a mixture of two fermionized Bose gases has similarities with a two component Fermi gas.)

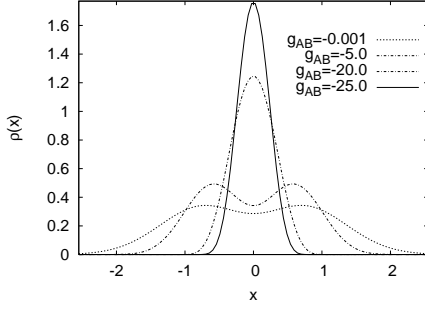


Figure 1: One-body density $\rho(x) \equiv \rho^{(\alpha)}(x)$ ($\alpha \in \{A, B\}$) for a quasi-fermionized mixture ($g_\sigma = 25.0$) with the particle numbers $N_\sigma = 2$, plotted for different inter-species interactions g_{AB} (see legend).

The characteristic fermionic pattern of the TG-state is displayed in the one-body density (that is the same for both species α for symmetry reasons) $\rho(x) = \rho^{(\alpha)}(x)$ (with $\alpha \in \{A, B\}$), which measures the probability distribution of finding one particle of the sort α at the position x pictured in Fig. 1. One recognizes the density concentrating more and more in the center of the trap with increasing inter-species attraction g_{AB} . Concurrently, in the intermediate interaction regime $|g_{AB}| = 5$ the initial two density peaks are at first getting increasingly pronounced, whereas the density in the center of the trap grows slowly. That intensification of the fermionic characteristic is due to molecule formation, as discussed in the following. In the very high interaction regime ($|g_{AB}| = 20 \sim g_\alpha$) the two peaks merge into one single peak in the center of the trap.

A more detailed insight in the systems behavior is given by the two-body correlation functions. In the case of a binary mixture, these are defined as

$$\rho_{\alpha\alpha}(x_1, x_2) = \frac{1}{N_\alpha(N_\alpha-1)} \langle \hat{\Psi}_\alpha^\dagger(x_1) \hat{\Psi}_\alpha^\dagger(x_2) \hat{\Psi}_\alpha(x_2) \hat{\Psi}_\alpha(x_1) \rangle$$

$$\rho_{AB}(x_A, x_B) = \frac{1}{N_A N_B} \langle \hat{\Psi}_A^\dagger(x_A) \hat{\Psi}_B^\dagger(x_B) \hat{\Psi}_B(x_B) \hat{\Psi}_A(x_A) \rangle$$

The two-body correlation functions $\rho_{\alpha\alpha}(x_1, x_2)$ and $\rho_{AB}(x_A, x_B)$ in Fig. 2, depict the conditional probability of measuring the one α -particle at the position x_1 and the other at the position x_2 , and likewise for the different species, $\rho_{AB}(x_A, x_B)$. The left column in Fig. 2 indicates that the two species keep their “fermionic” character, i.e., the probability of finding particles of the same kind at the same position $\{x_1 = x_2\}$ stays very low up to high inter-species attractions ($|g_{AB}| \lesssim 20$). But according to $\rho_{AB}(x_A, x_B)$ (right column), the two species concentrate more and more at the same position, which means on the diagonal in two separate peaks aside the center of the harmonic trap (see Fig. 2, $\rho_{AB}(x_A, x_B)$ for $g_{AB} = -5.0$). This can be understood as formation of a *molecular Tonks-Girardeau* (MTG) state: As we shall argue below, two distinguishable particles form a bound state, that is a molecule (in the following denoted as *AB-molecule*). These indistinguishable *AB-molecules* in turn form a Tonks-Girardeau state, a MTG state (see below). Whereas for two-component Fermi gases this molecular

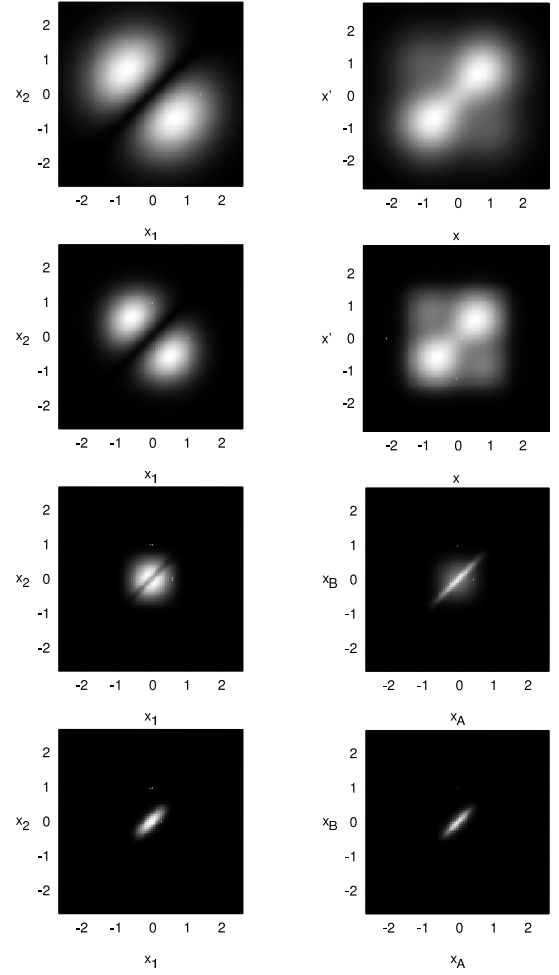


Figure 2: Two-body correlation functions $\rho_{\alpha\alpha}(x_1, x_2)$ (left column) and $\rho_{AB}(x_A, x_B)$ (right column) of two quasi-fermionized components $g_A = g_B = 25.0$ for inter-species couplings $g_{AB} = -0.01, -5.0, -20.0, -30.0$ (form top to bottom).

Tonks-Girardeau state remains stable even in the strongly attractive inter-species attraction regime [34], this is not the case in a pure bosonic mixture (see also Fig. 2).

Pairing description

For a better understanding of this behavior we examine the Hamiltonian for the exemplary case $N_\alpha = 2$. To this end, we transform $X \equiv (x_{A1}, x_{A2}, x_{B1}, x_{B2})^\top$ to the relative coordinates $Y = (R_{CM}, R_1, r_1, r_2)^\top$ specified by

$$Y = \mathcal{O}X, \quad \mathcal{O} = \begin{pmatrix} \frac{1}{\sqrt{4}} & \frac{1}{\sqrt{4}} & \frac{1}{\sqrt{4}} & \frac{1}{\sqrt{4}} \\ \frac{1}{2} & -\frac{1}{2} & \frac{1}{2} & -\frac{1}{2} \\ \frac{1}{\sqrt{2}} & 0 & -\frac{1}{\sqrt{2}} & 0 \\ 0 & \frac{1}{\sqrt{2}} & 0 & -\frac{1}{\sqrt{2}} \end{pmatrix}. \quad (3)$$

The coordinates $R_{CM}(r_1, r_2)$ coincide - up to a factor - with the standard center-of-mass (intra-species relative) coordi-

nates. The coordinate $R_1 = \frac{1}{2}[(x_{A_1} + x_{B_1}) - (x_{A_2} + x_{B_2})]$ specifies the distance between the centers of mass of two (A, B) -clusters. The orthogonal transformation leads to the Hamiltonian $H(Y) = h_{CM}(R_{CM}) + H_{rel}$, with

$$H_{rel} = \left[\frac{1}{2}p_{R_1}^2 + \frac{1}{2}R_1^2 \right] + \left[\sum_{i=1}^2 \frac{1}{2}p_{r_i}^2 + \frac{1}{2}r_i^2 + \frac{g_{AB}}{\sqrt{2}} \sum_{i=1}^2 \delta(r_i) \right] + g_A \delta\left(\frac{1}{\sqrt{2}}(r_1 - r_2) - R_1\right) + g_B \delta\left(\frac{1}{\sqrt{2}}(r_1 - r_2) + R_1\right) + g_{AB} \sum_{\pm} \delta\left(\frac{1}{\sqrt{2}}(r_1 + r_2) \pm R_1\right). \quad (4)$$

If we assume the formation of, say, $A_i B_i$ -bound states ($i \in \{1, 2\}$) (up to permutation symmetry), for high enough inter-species attraction g_{AB} the length scale within an $A_i B_i$ -molecule is much smaller than the distances between two such molecules ($|r_{1,2}| \ll |R_1|$). One can check this in the two-body correlation functions Fig. 2. In this limit, we can approximate (4) by the decoupled Hamiltonian

$$H_{rel} \approx \sum_{i=1}^2 \left[\frac{1}{2}p_{r_i}^2 + \frac{1}{2}r_i^2 + \frac{g_{AB}}{\sqrt{2}} \delta(r_i) \right] + \left[\frac{1}{2}p_{R_1}^2 + \frac{1}{2}R_1^2 + \tilde{g} \delta(R_1) \right], \quad (5)$$

with the last part describing the relative motion of the two AB -molecules with the effective interaction $\tilde{g} \equiv g_A + g_B + 2g_{AB}$. The analytic solution of the ground state is known [44] and the relative part can be written (excluding the trivial CM factor) as [19]

$$\psi_{rel}(X) \propto S_+ \left\{ \left(\prod_{i=1,2} e^{-\frac{|g_{AB}|}{2}|x_{A_i} - x_{B_i}|} \right) \times U\left(-\epsilon(\tilde{g}), \frac{1}{2}[(x_{A_1} + x_{B_1}) - (x_{A_2} + x_{B_2})]\right) \right\}, \quad (6)$$

where $\epsilon(\tilde{g}) = \nu(\tilde{g}) + 1/2$ is determined by the transcendental equation $\nu(g) \in f_g^{-1}(0) : f_g(\nu) := 2^{3/2} [\Gamma(\frac{1-\nu}{2}) / \Gamma(-\frac{\nu}{2})] + g$ and $U(a, b)$ denote the parabolic cylinder functions. The symmetry operator $S_+ := S_+^A \otimes S_+^B$ serves to compensate the symmetry breaking introduced in the Hamiltonian (5).

This solution gives a good approximation of the density patterns in Fig. 2 for intermediate to strong attractions ($|g_{AB}| < g_\alpha/2$). Also in the high coupling regime ($|g_{AB}| > g_\alpha/2$) the model provides applicable predictions for the system's behavior. Considering the molecule-molecule interaction term $\tilde{g} \delta(R_1) \equiv (g_A + g_B + 2g_{AB}) \delta(R_1)$, with large enough inter-species attraction g_{AB} the effective molecule-molecule interaction \tilde{g} vanishes and even becomes negative, i.e. attractive. That implies, more precisely, that for $g_{AB} \approx g_\alpha/2$ a state forms where the AB -molecules are condensed similar to a Bose-Einstein condensate (BEC). For further increase of the interaction, the gas of AB -molecules collapses and forms a bound state. Even though the introduced approximation model gives reasonable predictions in that limit of very high inter-species attractions ($|g_{AB}| > g_\alpha/2$), it should be handled with care, as the length scales are getting

comparable and therefore the scale separation breaks down (see also Fig. 2).

These conceptions can be supported by means of the quantities of the one-body density matrix $\rho_1^{(\alpha)}(x, x') = \frac{1}{N_\alpha} \langle \hat{\Psi}_\alpha^\dagger(x) \hat{\Psi}_\alpha(x') \rangle$ and the pair density matrix - where composite particles play the role of elementary objects- defined as

$$\tilde{\rho}(x, x') := \frac{1}{N_A N_B} \langle \Delta_{AB}^\dagger(x) \Delta_{AB}(x') \rangle,$$

with the “pair” operator $\Delta_{AB}(x) \equiv \hat{\Psi}_A(x) \hat{\Psi}_B(x)$, that annihilates an AB -pair “particle” at the position x . As $|\Delta_{AB}(x) \Psi\rangle$ is a “hole”-state, i.e. a state where an AB -pair has been removed at the position x , the pair density matrix embodies the overlap of two such “hole”-states. The pair density matrix reflects the correlation inherent in the state Ψ between the positions x and x' on the level of AB -dimers, as opposed to correlations of single particles α described by $\rho_1^{(\alpha)}(x, x')$.

As shown in Fig. 3, the off-diagonal range of the pair density matrix $\tilde{\rho}(x, x')$ persists and even slightly increases for the inter-species attractions up to $|g_{AB}| \approx 5$, where its appearance agrees well with the corresponding one-body density matrix $\rho_1^{(M)}(x, x')$ of identical, fermionized bosons with mass $M = 2$ (in units of m). This proves the existence of a paired state (MTG), as discussed above. For intermediate attractions ($|g_{AB}| < g_\alpha/2$), the single-particle density matrix $\rho_1^{(\alpha)}(x, x')$ (see Fig. 3 left column) shows two peaks on the diagonal, while the off-diagonal density steadily diminishes with increasing $|g_{AB}|$. In this light a single α -atom will be in an incoherent superposition of left- (right-) localized states, without any phase correlations. This has to be contrasted with the phase correlations present for the pair density matrix (see Fig. 3 right column for $g_{AB} = -5.0$). Interestingly this may be compared to a demixed state in the presence of repulsive inter-species interactions [26].

When further increasing the inter-species interaction to $|g_{AB}| \approx 20$ the size of the system decreases; however, a seemingly perfect off-diagonal long range order [45] in the pair density matrix is attained, which can be interpreted as (few-body analog of) of *condensed state* on the level of AB -molecules, $\tilde{\rho}(x, x') = \varphi_{AB}^*(x) \cdot \varphi_{AB}(x')$ (see Fig. 3 right column for $g_{AB} = -20.0$). By contrast, on the single-particle level, displayed in the one-body density matrix $\rho_1^{(\alpha)}(x, x')$, no condensed state exists, but the two correlation peaks merge into one centered peak concentrated on the diagonal $\{x = x'\}$.

For inter-species interaction strength larger than the order of magnitude of the intra-species interactions $|g_{AB}| \gg |g_\alpha|/2$ the system becomes highly bound beyond the AB -molecule level, as is reflected in the decrease of the off-diagonal elements in the pair density matrix $\tilde{\rho}(x, x')$. This can be seen as a *collapse* from a molecular gas to a strongly interacting cluster of AB -molecules. In contrast to a Bose-Fermi [37] and Fermi-Fermi mixture [34] the collapse in a pure bosonic mixture is qualitatively different: In a Bose-Fermi mixture only the bosons form a small region with high density, whereas the fermions will be attracted up to a “Pauli-

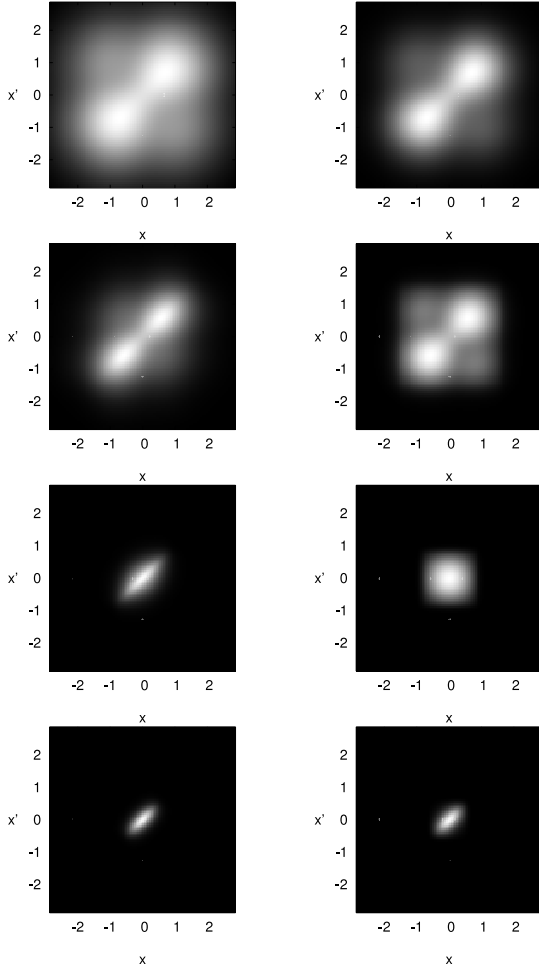


Figure 3: One-body density matrix $\rho_1(x, x')$ (left column) and pair density matrix $\tilde{\rho}(x, x')$ (right column) for inter-species couplings $g_{AB} = -0.01, -5.0, -20.0, -30.0$ (from top to bottom).

allowed” density, and Fermi-Fermi mixtures with s -wave interactions remain mechanically stable even in the strongly attractive inter-species regime.

Although, for definiteness, we restricted our discussion to a mixture with particle numbers $N_\alpha = 2$, the mechanism is expected to extend to higher particle numbers and the condensation occurs at similar inter-species interaction strength g_{AB} .

Attractive components

It is known for identical bosons that fermionization can also be obtained in the attractive interaction regime [17, 19], where it is called the *super-Tonks-Girardeau* state (STG). We show that the above pairing mechanism can also be observed in a mixture with two attractively interacting, fermionized components ($g_\alpha < 0$, $\alpha \in \{A, B\}$). In this case it is no longer the ground state but an excited state of the system. We performed the numerical investigation for the exemplary case of a mixture with $N_\alpha = 2$ being situated in the energetically

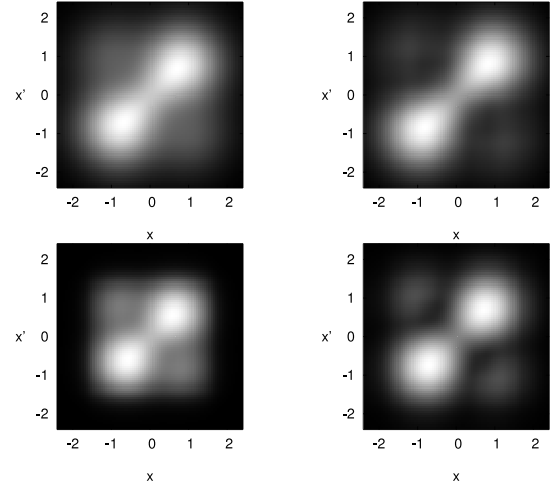


Figure 4: Pair density matrix $\tilde{\rho}(x, x')$ for $g_\alpha = 25.0$ (left column) and the super-Tonks-Girardeau state $g_\alpha = -15.0$ (right column) ($\alpha \in \{A, B\}$). The inter-species interaction parameters are $g_{AB} = -0.01, -5.0$ (from top to bottom).

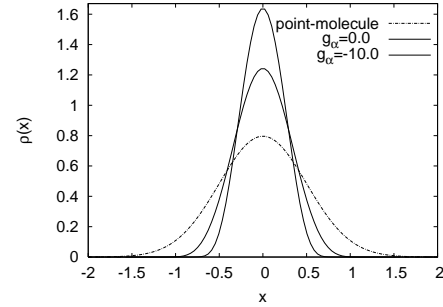


Figure 5: One-body density $\rho(x)$ of $\frac{N}{2} = 2$ point-like molecules of mass $M = 2$ with interaction strength $\tilde{g} = 0$ (dashed), two non-interacting components with $g_{AB} = -10.0$ (solid thin), and two molecular components with $g_{AB} = -10.0$ (solid thick).

lowest STG-state ($g_\alpha = -15.0$). Direct comparison with a system of repulsive, fermionized components shows the corresponding process analogous to the formation of the molecular TG-gas, but with a smaller off-diagonal correlations (Fig. 4). Obviously the density profile of the STG-state is more localized in fragmented regions than that of the TG-state (Fig. 4). The reason is the finite intra-species interaction-strength (here $g_\alpha = -15.0$), where the state is not completely fermionized. Since this quasi-STG-state still has a non-vanishing, positive 1D-scattering length $a_\alpha = -\frac{2}{g_\alpha} > 0$, it is closer to a gas of spatially extended, hard-core particles (so-called hard rods) than to a completely fermionized, point-like TG-gas, and localization effects are more pronounced, which can be observed in the more profiled density.

B. Weakly interacting components

Following the pathway to weak intra-species repulsion, the mechanism of pair formation is getting constantly weaker till it vanishes in the weak-interaction regime ($g_\alpha \sim 1$). In this weakly interacting regime we turn to the limit case of two hardly interacting, BEC-like components ($g_\alpha \approx 0$). Compared to the case of two strongly repulsive components, there is no formation of a condensed state of AB -molecules, but the system collapses with the increase of the inter-species attraction. In other words, between the AB -molecules there is always an effective attractive interaction and thus for strong interaction a bright-soliton-like state evolves. Figure 5 displays a comparison of the one-body densities of (i) two identical point-molecules each of mass $M = 2$, which mirrors the case of very tightly bound, point-like AB -molecules with no molecular interaction $\tilde{g} = 0$, (ii) an N -body bound state of the form

$$\Psi(X) \propto \Phi_0(R) \left\{ e^{-\frac{|g_{AB}|}{2} \left(\sum_{i,j \leq 2} |x_{A_i} - x_{B_j}| \right)} \prod_{\alpha \in \{A,B\}} e^{-\frac{|g_\alpha|}{2} |x_{\alpha_1} - x_{\alpha_2}|} \right\}$$

and (iii) the case $g_\alpha = 0$, which is a solitonic state in between the two extremes.

We note that the coherence between the “ AB -molecules” (as evidenced in the pair density matrix) is slightly stronger compared to the one-body level $\rho_1^{(\alpha)}(x, x')$, as there is just explicit interaction between the species (g_{AB}). However, as there is no longer a scale separation, one cannot consider this system simply as a gas of point-like molecules.

C. Imbalanced Components

After having studied the mechanism for equal component settings, we now want to highlight the effects of relaxing the equality of the particle numbers and the intra-species interaction strengths.

Unequal particle numbers

We first consider the case of unequal particle numbers $N_A \neq N_B$, but still the same intra-species interaction strengths ($g_A = g_B$). We picture this by means of the case of two quasi-fermionized species ($g_\alpha = 25.0$) with particle numbers $N_A = 3$ and $N_B = 2$. On the way from weak to very strong inter-species attractions g_{AB} , an analogous progression occurs as for fermionized binary mixtures with equal particle numbers, as can be checked on the basis of the pair density matrix. That is, a MTG state forms in the intermediate inter-species interaction regime, followed by condensation and collapse for even higher inter-species attractions. The effect of the difference in the particle numbers (or particle densities) can be seen as a formation of two phases, i.e. the one consists of tightly bound AB -molecules, as in the case of equal

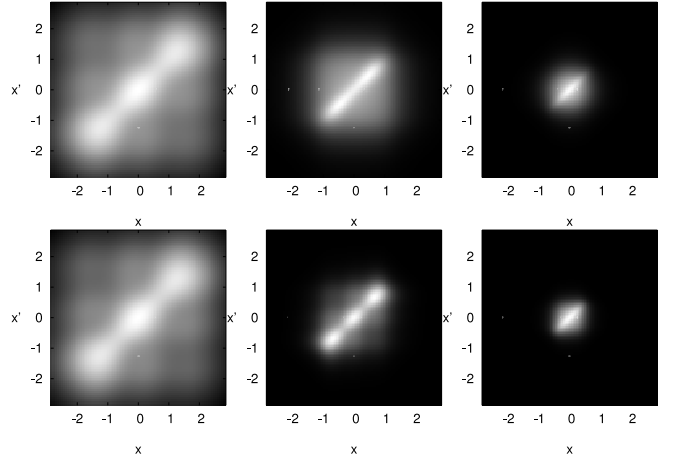


Figure 6: One-body density matrix $\rho_1^{(A)}(x, x')$ of two quasi-fermionized components ($g_\alpha = 25.0$) for the inter-species interaction strength $g_{AB} = -0.01, -10.0, -20.0$ (from left to right) of a mixture with particle numbers $N_A = 3$ and $N_B = 2$ (upper row), $N_A = N_B = 3$ (lower row).

species numbers, and the other consists of N_d “loosely bound” spare particles, where $N_d \equiv |N_A - N_B|$ (here: $N_d = 1$), i.e. particles that are hardly affected by the inter-species interaction. (Of course, this picture has to be viewed from the perspective of taking into account the proper particle exchange symmetries.) This picture of loosely bound particles provides a good understanding of the two-body density patterns in the intermediate to strong inter-species interaction regime ($|g_{AB}| \lesssim 10$). Furthermore this formation of, in this case, two AB -molecules and one loosely bound particle manifests in the one-body density matrix $\rho_1^{(A)}(x, x')$ (Fig. 6) in the formation of two density peaks on the diagonal $\{x' = x\}$ and the larger off-diagonal density compared to the balanced counterpart ($N_A = N_B = 3$), respectively. This two-phase picture breaks down as the system starts to collapse for larger attraction (see Fig. 6, $g_{AB} = -20$).

Unequal inter-species repulsions

Now we consider unequal intra-species repulsions $g_A \neq g_B$. For the sake of clarity, we keep the particle numbers equal $N_A = N_B$. We start with the case of all intra-species interactions corresponding to the fermionization regime, here $g_A = 10.0$ and $g_B = 25.0$. In the chosen example the species A is weakly fermionized, but still the system evolves similar to the case of two strongly fermionized species discussed above, that is we observe the formation of a pronounced Tonks-Girardeau pattern in the pair density matrix $\tilde{\rho}(x, x')$, indicating the MTG state. This is in line with Figure 7, which pictures the $\tilde{\rho}(x, x')$ -profile along the diagonal $\{x' = x\}$ and along the off-diagonal $\{x' = -x\}$.

During the formation of the MTG state, one can observe an assimilation of the profiles, for instance, of the one-body density matrices $\rho_1^{(A)}(x, x')$ and $\rho_1^{(B)}(x, x')$. Best profile assim-

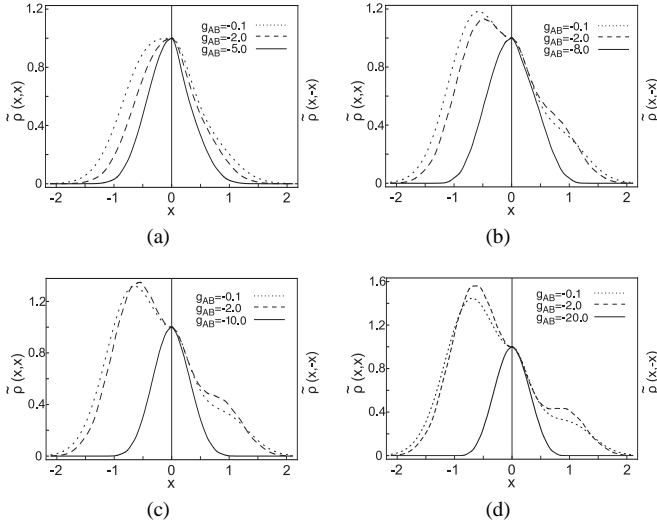


Figure 7: Pair density matrix $\tilde{\rho}(x, x')$ for the particle numbers $N_A = N_B = 2$ plotted along the diagonal $\{x' = x\}$ for $x \in [-2.2, 0.0]$ and along the off-diagonal $\{x' = -x\}$ for $x \in [0.0, 2.2]$, of one fermionized component $g_B = 25.0$ and intra-species interactions of the other component: (a) $g_A = 0.01$ (b) $g_A = 5.0$ (c) $g_A = 10.0$ (d) $g_A = 25.0$. The highest inter-species interaction (solid line) shows the best possible symmetry between on- and off-diagonal. (The densities have been rescaled to the same maximal value at the position $x = 0$.)

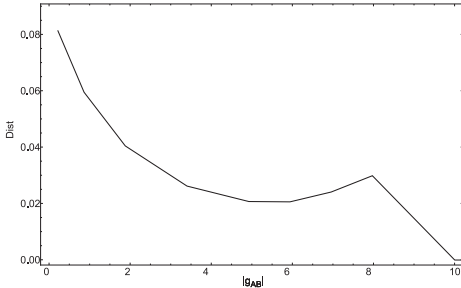


Figure 8: Distance Dist between the one-body density maxima $\text{Max}[\rho_1^{(\alpha)}(x, x')]$ of the components $\alpha \in \{A, B\}$ for different inter-species interaction strength g_{AB} and the intra-species interactions $g_A = 10.0$ and $g_B = 25.0$.

ilation is achieved about the value $|g_{AB}| \approx 5.0$. To characterize this increasing similarity of the two profiles, let us define the distance between the peak positions of each component (where the diagonal density $\rho_1^{(\sigma)}(x^{(max,\sigma)}, x^{(max,\sigma)})$ is maximal), which for a given inter-species coupling g_{AB} is given by $\text{Dist} := |x^{(max,A)} - x^{(max,B)}|$ (see Fig. 8).

With a further increase of the inter-species interaction ($|g_{AB}| > 5$), the system collapses in a way characteristic for Bose-Fermi mixtures [37]. That is, the component A with the less fermionic character forms a high density region in the center of the trap, whereas the strongly fermionized component keeps its fermionic character up to higher inter-species interactions ($|g_{AB}| \approx 8.0$). That decrease of the density adaption is visualized in the light increase of the distance Dist

of the extrema of the one-body density for $5 < |g_{AB}| \lesssim 8$ (Fig. 8). This characteristic does not hold for very high inter-species interactions ($|g_{AB}| \gtrsim 10$), where the system collapses according to that of two equally fermionized Bose components, discussed above. The comparison of the case at hand (see Fig. 7 (c)) with that of two fermionized components (see Fig. 7 (d)) shows, that the scale of the off-diagonal profiles are always smaller than that of the diagonal profiles. Thus no g_{AB} exists for which a perfect off-diagonal long range order is achieved in the pair density matrix $\tilde{\rho}(x, x')$. In this sense, the system starts to collapse, without forming a condensed state on the AB -molecule level. Noteworthy, if both components are equally weakly fermionized ($g_A = g_B = 10.0$), no segregative collapse occurs as in the above case, and a condensed state can be observed.

Going towards components with intermediate and weak intra-species repulsions (like $g_A \lesssim 5$ shown in Fig. 7 (a) and (b)) the pair-formation is not visible anymore, and the system immediately starts to collapse without forming a condensed state as in the case before. In the extreme case of one “condensed” component ($g_A \rightarrow 0^+$), the approximation (5) above is not valid as the length scales cannot be separated anymore. For unequal particle numbers, the system can again be thought of as a two-phase system; hence if the particle number of the fermionized state (say B) exceeds the number of condensed particles, the coherence in the one-body density $\rho_1^{(B)}(x, x')$ has larger off-diagonal elements due to spare (unbound) B -particles.

III. MIXTURE WITH ATTRACTIVE COMPONENTS

In this section we complete our investigation by exploring mixtures with attractively interacting components ($g_\alpha < 0$).

A. Repulsive and attractive components

We start in the spirit of the above section with one component in the fermionized interaction limit, i.e. $g_B = 25.0$ and the other in a bound state $g_A = -10.0$. The bound species are strongly localized in the center of the trap and the feedback on that component during the increase of the inter-species attraction is negligible. To explore this situation it is natural to consider a simplified Hamiltonian, where the effect of the localized species A is replaced by an additional external potential for the B atoms $\mu(x) = g_{AB}N_A\delta(x)$. Here we apply the analytically well studied split-trap [46, 47],

$$\begin{aligned} \bar{H}_B = & \sum_{i=1}^{N_B} \left(\frac{1}{2} p_{B_i}^2 + \frac{1}{2} x_{B_i}^2 + 2g_{AB}\delta(x_{B_i}) \right) \\ & + g_B \sum_{i < j}^{N_B} \delta(x_{B_i} - x_{B_j}). \end{aligned} \quad (7)$$

Furthermore for $g_B \gg 1$, one can map the fermionized component on a *non-interacting* fermionic system [9]. Consequently one obtains for the exemplary case of $N_B = 2$

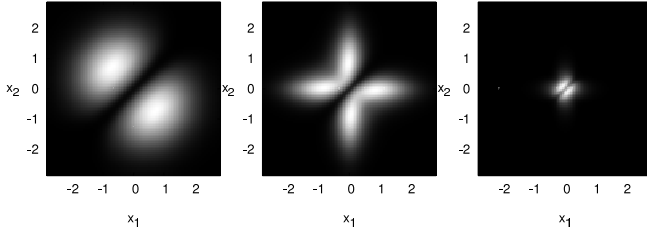


Figure 9: Two-body correlation function $\rho_{BB}(x_1, x_2)$ of a mixture with one molecular species $g_A = -10.0$ ($N_A = 4$) and one species of $N_B = 2$ repulsive bosons, $g_B = 25.0$, for the inter-species interaction parameter $g_{AB} = -0.01, -1.0, -5.0$ (from left to right).

B -particles the simple solution $\Psi_0^{Boson} = |\Psi_0^{Fermion}| = \frac{1}{\sqrt{2}} |\Phi_0(x_1)\Phi_1(x_2) - \Phi_0(x_2)\Phi_1(x_1)|$, where Φ_i denotes the i -th single-particle eigenstate of a split-trap.

The validity of the approximation becomes rapidly better with increasing number of particles (N_A) in the bound state, as the width of one-body density $\rho^{(A)}(x)$ scales as $\frac{1}{\sqrt{N_A}}$, and hence converges towards a δ -type potential in the limit of large particle numbers ($N_A \rightarrow \infty$). The agreement is astonishingly good already with relatively few particles $N_A \geq 4$. In Fig. 9, the exact two-body correlation function $\rho_{BB}(x_1, x_2)$ for $N_B = 2$ particles is shown. As it turns out, the picture of a non-interacting fermionic system applies very well up to intermediate inter-species interactions $|g_{AB}| < 2$ (in the case of $N_A = 4$). This predicts that if for intermediate inter-species interaction $g_{AB} \approx -1$ one detects a B -particle aside the trap center ($x_{B_1} \approx \pm 1$), the other B -particle is located at the center of the trap ($x_{B_2} \approx 0$). (For $N_B > 2$ an additional density contribution emerges on the off-diagonal.)

Whereas for the model δ -type potential the two-body density $\rho_{BB}(x_1, x_2)$ would remain in the (increasingly sharp) cross-shaped pattern even for $g_{AB} \rightarrow -\infty$, this is not the case for the system at hand (see Fig. 9 for $g_{AB} = -5.0$). Due to the nonzero width of the additional potential caused by the A -particles, for high enough inter-species attraction all of the B particles can be accommodated in the “ A -potential” as a whole (unlike for a δ -type potential). That is illustrated in Fig. 9 for $g_{AB} = -5.0$, where again the familiar TG-density pattern can be observed, but with the spatial extension of the A -particle density (compare with Fig. 10). This behavior in the high interaction regime can also be observed for higher B -particle numbers.

B. Two attractive components

Extending the results of the last section, we start with the case of one weakly interacting, i.e. condensed component ($g_B \approx 0$), and the other component again in a bound state ($g_A = -10.0$). We can again apply the previous split-trap approximation on a system with $N_B = 2$, i.e. the condensed B -particle feel an effective short-range potential at the center of the harmonic trap. Again with increasing particle-number N_A in the molecular state, the approximation is getting better. However, for the length scales of the two components to

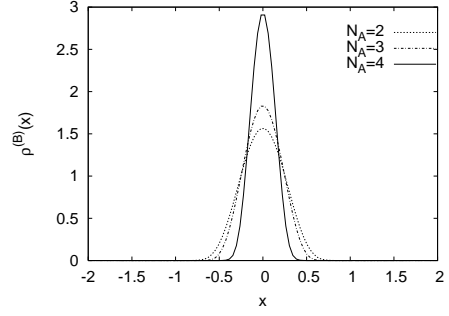


Figure 10: One-body density $\rho^{(B)}(x)$ of $N_B = 2$ non-interacting B -particles ($g_B = 0.0$), with different A -particle numbers N_A in a bound state ($g_A = -10.0$) and the inter-species interaction strength $g_{AB} = -10.0$.

differ as distinctly as in the case of a fermionized component, the agreement with the split-trap model above requires more B -particle in the bound state. If we assume as a model a condensed state in component B ($g_B = 0$) and a tightly bound, δ -type state in component A , the model Hamiltonian (7) reduces to

$$\bar{H}_B = \sum_{i=1}^2 \left(\frac{1}{2} p_{B_i}^2 + \frac{1}{2} x_{B_i}^2 + 2g_{AB} \delta(x_{B_i}) \right), \quad (8)$$

with the solution [47]

$$\Psi_0(X_B) \propto \exp\left(-\frac{(x_{B_1}^2 + x_{B_2}^2)}{2}\right) \prod_{i=1}^{N_A} U\left(\frac{1}{2} - \frac{E_0}{2}, \frac{1}{2}, x_{B_i}^2\right),$$

which evolves with increasing inter-species attraction towards a state analogous to the bound state of the δ -potential.

For higher attractive interactions also in component B , the model is not applicable anymore. In the limit of highly attractive components, with increasing inter-species interaction strength the system forms an entire bound state. For the special case of equal interaction strength $g_A = g_B = g_{AB} \equiv g$ one can map the system on a bound state of $N_A + N_B$ identical particles $\Psi_0(X \equiv (X_A, X_B)) \propto \Phi_0(R) \exp\left(-\frac{|g|}{2} \sum_{i < j} |x_i - x_j|\right)$.

IV. SUMMARY

In conclusion, we have investigated the ground state of a two-component Bose gas in a one-dimensional harmonic trap throughout the crossover from weak to strong inter-component attraction. We have highlighted different pathways depending on the choices of the different intra-component couplings, and indicated how they can be understood in terms of simplified models. For two quasi-fermionized components (i.e. Tonks-Girardeau states), the system forms a molecular Tonks-Girardeau gas in the intermediate inter-component interaction regime, which consists of bound pairs containing one particle of each component. In

the strongly attractive regime, we demonstrated the condensation of the bound pairs, followed by the collapse of the system beyond a critical attraction. We showed the analogous mechanism for attractively fermionized components, that is components in the super-Tonks-Girardeau regime. Relaxation of the condition of two equally fermionized components leads to a modified pathway: In the case of just one fermionized component, the formation of a molecular Tonks-Girardeau gas can still be observed for high enough repulsion within the second component, but the collapse occurs in analogy to Bose-Fermi mixtures without condensation of the bound pairs, in contrast to the case of comparable repulsions. In the regime of intermediate (inter-species) attraction, unequal (number-) densities in the components have been found. These can be understood as two phases, one consisting of molecular pairs of each component, and the other phase consisting of loosely bound particles. For mixtures with one strongly attractive component,

we showed that this component can be interpreted as an additional external δ -function potential for the other component, in case both length scales can be well separated. The study of these intriguing pairing scenarios pave the way toward studying their quantum dynamics, such as the tunneling of molecular pairs in multi-well traps.

Acknowledgments

Financial support from the Landesstiftung Baden-Württemberg through the project “Mesoscopics and atom optics of small ensembles of ultracold atoms” is gratefully acknowledged by P.S. and S.Z. We thank H.-D. Meyer, X.-W. Guan, and O. Alon for fruitful discussions.

-
- [1] I. Bloch, J. Dalibard, and W. Zwerger, *Rev. Mod. Phys.* **80**, 885 (2008).
 - [2] M. Lewenstein *et al.*, *Adv. Phys.* **56**, 243 (2007).
 - [3] T. Köhler, K. Góral, and P. S. Julienne, *Rev. Mod. Phys.* **78**, 1311 (2006).
 - [4] S. Giorgini, L. P. Pitaevskii, and S. Stringari, *Rev. Mod. Phys.* **80**, 1215 (2008).
 - [5] E. H. Lieb and W. Liniger, *Phys. Rev.* **130**, 1605 (1963).
 - [6] M. Olshanii, *Phys. Rev. Lett.* **81**, 938 (1998).
 - [7] T. Kinoshita, T. Wenger, and D. S. Weiss, *Science* **305**, 1125 (2004).
 - [8] B. Paredes *et al.*, *Nature* **429**, 277 (2004).
 - [9] M. Girardeau, *J. Math. Phys.* **1**, 516 (1960).
 - [10] O. E. Alon and L. S. Cederbaum, *Phys. Rev. Lett.* **95**, 140402 (2005).
 - [11] Y. Hao, Y. Zhang, J. Q. Liang, and S. Chen, *Phys. Rev. A* **73**, 063617 (2006).
 - [12] S. Zöllner, H.-D. Meyer, and P. Schmelcher, *Phys. Rev. A* **74**, 053612 (2006).
 - [13] S. Zöllner, H.-D. Meyer, and P. Schmelcher, *Phys. Rev. A* **74**, 063611 (2006).
 - [14] F. Deuretzbacher, K. Bongs, K. Sengstock, and D. Pfannkuche, *Phys. Rev. A* **75**, 013614 (2007).
 - [15] B. Schmidt and M. Fleischhauer, *Phys. Rev. A* **75**, 021601 (2007).
 - [16] J. B. McGuire, *J. Math. Phys.* **5**, 622 (1964).
 - [17] G. E. Astrakharchik, J. Boronat, J. Casulleras, and S. Giorgini, *Phys. Rev. Lett.* **95**, 190407 (2005).
 - [18] M. T. Batchelor, M. Bortz, X. W. Guan, and N. Oelkers, *J. Stat. Mech.* **2005**, L10001 (2005).
 - [19] E. Tempfli, S. Zöllner, and P. Schmelcher, *New J. Phys.* **10**, 103021 (2008).
 - [20] C. J. Myatt *et al.*, *Phys. Rev. Lett.* **78**, 586 (1997).
 - [21] J. Stenger *et al.*, *Nature* **396**, 345 (1998).
 - [22] S. B. Papp, J. M. Pino, and C. E. Wieman, *Phys. Rev. Lett.* **101**, 040402 (2008).
 - [23] T. Fukuhara, S. Sugawa, Y. Takasu, and Y. Takahashi, *Phys. Rev. A* **79**, 021601 (2009).
 - [24] G. Modugno *et al.*, *Phys. Rev. Lett.* **89**, 190404 (2002).
 - [25] M. D. Girardeau and A. Minguzzi, *Phys. Rev. Lett.* **99**, 230402 (2007).
 - [26] S. Zöllner, H.-D. Meyer, and P. Schmelcher, *Phys. Rev. A* **78**, 013629 (2008).
 - [27] Y. Hao and S. Chen, *Eur. Phys. J. D* **51**, 261 (2009).
 - [28] Y. Hao, Y. Zhang, X.-W. Guan, and S. Chen, *arXiv:0811.1065*.
 - [29] O. E. Alon, A. I. Streltsov, and L. S. Cederbaum, *Phys. Rev. Lett.* **97**, 230403 (2006).
 - [30] T. Mishra, R. V. Pai, and B. P. Das, *Phys. Rev. A* **76**, 013604 (2007).
 - [31] T. Roscilde and J. I. Cirac, *Phys. Rev. Lett.* **98**, 190402 (2007).
 - [32] A. Kleine *et al.*, *Phys. Rev. A* **77**, 013607 (2008).
 - [33] M. A. Cazalilla and A. F. Ho, *Phys. Rev. Lett.* **91**, 150403 (2003).
 - [34] G. E. Astrakharchik, D. Blume, S. Giorgini, and L. P. Pitaevskii, *Phys. Rev. Lett.* **93**, 050402 (2004).
 - [35] L. Salasnich, S. K. Adhikari, and F. Toigo, *Phys. Rev. A* **75**, 023616 (2007).
 - [36] L. Pollet, C. Kollath, U. Schollwöck, and M. Troyer, *Phys. Rev. A* **77**, 023608 (2008).
 - [37] M. Rizzi and A. Imambekov, *Phys. Rev. A* **77**, 023621 (2008).
 - [38] M. H. Beck, A. Jäckle, G. A. Worth, and H.-D. Meyer, *Phys. Rep.* **324**, 1 (2000).
 - [39] G. A. Worth, M. H. Beck, A. Jäckle, and H.-D. Meyer, The MCTDH Package, Version 8.2, (2000). H.-D. Meyer, Version 8.3 (2002), Version 8.4 (2007). See <http://www.pci.uni-heidelberg.de/tc/usr/mctdh/>.
 - [40] H.-D. Meyer, U. Manthe, and L. S. Cederbaum, *Chem. Phys. Lett.* **165**, 73 (1990).
 - [41] S. Zöllner, H.-D. Meyer, and P. Schmelcher, *Phys. Rev. A* **75**, 043608 (2007).
 - [42] S. Zöllner, H.-D. Meyer, and P. Schmelcher, *Phys. Rev. Lett.* **100**, 040401 (2008).
 - [43] M. Eckart *et al.*, *New J. Phys.* **11**, 023010 (2009).
 - [44] T. Busch, B. G. Englert, K. Rzazewski, and M. Wilkens, *Found. Phys.* **28**, 549 (1998).
 - [45] C. N. Yang, *Rev. Mod. Phys.* **34**, 694 (1962).
 - [46] T. Busch and G. Huyet, *J. Phys. B* **36**, 2553 (2003).
 - [47] J. Goold and T. Busch, *Phys. Rev. A* **77**, 063601 (2008).